AIMS Mathematics, 11(5): 15143–15162.
DOI: 10.3934/math.2026623
Received: 31 December 2025
Revised: 28 April 2026
Accepted: 08 May 2026
Published: 29 May 2026

https://www.aimspress.com/journal/Math

Research article

Distributed Hessian–Riemannian flow for multi-population wardrop equilibrium

Tigran Bakaryan[1,*], Christoph Aoun[2], Ricardo de Lima Ribeiro[3], Naira Hovakimyan[4] and Diogo Gomes[5]

[1] Institute of Mathematics NAS RA, Center for Scientific Innovation and Education, Yerevan State University, Yerevan, Armenia

[2] Department of Aerospace Engineering, University of Illinois at Urbana-Champaign, Urbana, IL 61801, USA

[3] Applied Mathematics and Computational Sciences, King Abdullah University of Science and Technology, 23955 Thuwal, Saudi Arabia

[4] Department of Mechanical Science and Engineering, University of Illinois at Urbana-Champaign, Urbana, IL 61801, USA

[5] Mathematics and Computational Sciences, King Abdullah University of Science and Technology, 23955 Thuwal, Saudi Arabia

* **Correspondence:** Email: tigran.bakaryan@instmath.sci.am.

Abstract: In this paper, we studied a multi-population Wardrop equilibrium on generalized directed graphs with heterogeneous costs. Using an edge-flow representation, we formulated the equilibrium as a variational inequality and provided sufficient conditions for existence and uniqueness under compactness, continuity, and monotonicity assumptions. We showed that the equilibrium problem is equivalent to a noncooperative game among the populations. Relying on this game formulation, we proposed a multi-population Hessian–Riemannian flow for computing the equilibrium. The flow exploited the geometry of the feasible flow space and preserved the Kirchhoff flow-conservation constraints. We proved convergence of the continuous-time dynamics under the stated assumptions and demonstrated the method on heterogeneous traffic examples through comparisons with benchmark methods, including projected gradient, Gauss–Seidel, and nonlinear programming, as well as through an emissions-related case study.

Keywords: Wardrop equilibrium; multi-population traffic; variational inequality; edge-flow formulation; Hessian–Riemannian flow; distributed computation
Mathematics Subject Classification: 90B20, 90C33, 91A43

1. Introduction

In traffic management, each driver—whether operating a car, SUV, or truck—selects the route they perceive to be the shortest. The resulting traffic distribution, in which no driver can unilaterally switch routes to reduce travel time or cost, is known as an equilibrium. For a homogeneous (single-population) flow, this equilibrium is formalized as the Wardrop equilibrium, as stated in the first Wardrop principle [6]:

"The journey times on all the routes actually used are equal and less than those which would be experienced by a single vehicle on any unused route."

While the classical Wardrop model assumes all users have an identical impact on congestion and perceive identical costs, real-world traffic systems are inherently heterogeneous: Different vehicle types contribute unequally to congestion and experience different costs. For instance, trucks may slow traffic more than cars, and their operators may evaluate travel costs differently. To account for these disparities, the Wardrop principle has been extended to multi-population settings, where each population represents a class of users with distinct characteristics and cost functions (see [8, 17], and references therein).

Motivated by the need to model more realistic traffic behavior, we investigates the multi-population Wardrop equilibrium using a variational inequality framework. This formulation arises naturally from the observation that, at equilibrium, users travel along the shortest paths with respect to the given cost. We discuss the existence and uniqueness of solutions to multi-population Wardrop equilibrium. Furthermore, we introduce a novel method to compute the solution efficiently.

Wardrop's first principle is often presented in a *path-based* language, where travelers compare the costs of complete routes and reallocate demand until no used route can be improved by unilateral switching [27]. Furthermore, congestion is generated by physical network elements, including links and junctions, where local interactions (merges, signals, turning movements, competing inflows) create delays that are not always captured cleanly by a simple path-additive structure. Moreover, a path-flow representation becomes computationally heavy because the set of relevant paths can grow rapidly with network size. To overcome these issues, in this paper, we follow Smith [22, 23] and work with an edge-flow representation of Wardrop equilibrium. The edge-flow representation avoids explicit path enumeration and can accommodate cost operators depending on local edge and junction-level flow interactions. Smith [22, 23] established the equivalence between path-wise and edge-wise Wardrop equilibria and proved existence and stability directly in terms of link flows.

In the literature, the definitions of Wardrop equilibrium and Nash equilibrium are often used interchangeably in the context of non-cooperative network games involving multiple populations. For example, in [10], the authors demonstrated that, under certain conditions defined by entrance-exit pairs and demand patterns, the asymptotic behavior of the Nash–Cournot equilibrium converges to a Wardrop equilibrium. Existence and uniqueness of equilibria are central to network optimization problems. In [20], it is shown that, in nearly parallel networks, the Nash equilibrium is topologically unique. Conversely, the researchers in [5] pointed out that atomic game equilibria, while existent, are not necessarily unique. Further, the researchers in [17] established conditions, specifically, diagonal strict convexity (DSC), as derived from [21], that guarantee the existence and uniqueness of a Nash equilibrium for multi-player flows on generalized networks. Inspired by [17], the authors in [1] also derived similar conditions for competitive polynomial cost functions. In this paper, we employ

conditions analogous to those in [17, 25] to demonstrate the uniqueness of our resulting equilibrium. These DSC conditions can be interpreted as a form of strict monotonicity of the underlying variational inequalities, as will be discussed in Section 5.

Facchinei and Kanzow [7] provided a broad survey of generalized Nash equilibrium problems, emphasizing their connection with variational inequalities and reviewing several classes of numerical methods, in particular Newton-type and penalty-based approaches. In a more specific equilibrium setting, Paccagnan et al. [19] studied aggregative games with coupling constraints, characterized Nash and Wardrop equilibria through variational inequalities, and proposed decentralized algorithms converging to these equilibria. Related numerical and structural perspectives also appear in the work of Wang and Jia [28], who studied a generalized Nash equilibrium problem with inequality constraints and proposed a numerical solver with convergence analysis, and in [24], which investigated the existence and uniqueness properties for linear complementarity problems over tensor spaces. These works motivate the use of variational inequalities and game-theoretic tools; however, we differ by combining a multi-population edge-flow Wardrop formulation with Hessian–Riemannian dynamics that preserve Kirchhoff constraints. The population-indexed formulation may also be viewed as a multilayer network in which each population defines a flow layer and the layers interact through shared congestion costs; related multilayer game-theoretic perspectives appear, for example, in [13].

Once the existence and uniqueness of an equilibrium have been established, the next step is to develop an algorithm capable of efficiently computing the equilibrium in multi-player network games. Several computational approaches have been proposed when the equilibrium is characterized via a minimization principle. For example, a Gauss-Seidel approach, which iteratively fixes the flows of all but one player and then optimizes the remaining player's flow using the fixed values from the others [3]. In [14], the authors show that such an algorithm converges to the equilibrium provided that inter-class interactions are relatively weak compared to the primary effects, evidenced by cost function Jacobian norms being less than one. However, many multi-population problems involve highly coupled cost functions, limiting the applicability of this approach. Furthermore, in [15], the multi-class networking problem was tackled by assuming affine cost functions and reformulating the system as a linear complementarity problem, which was then solved via a Lemke-like algorithm. Despite its theoretical appeal, this method has been found to be unscalable, the computational time increases exponentially with the size of the network and the number of populations. To address this [16] extended the Lemke-like algorithm by leveraging properties of hyperplane arrangements, resulting in a polynomial-time solution. However, these methods either cannot be directly applied to our variational case, converge under strong assumptions, or have a high computational and time cost. In this paper, by leveraging the Hessian–Riemannian flow (HRF) (see [2, 9]), we develop an algorithm to find multi-population Wardrop equilibrium. Particularly, we first establish that the multi-population Wardrop equilibrium problem is equivalent to a noncooperative game among the populations. Then, based on this game formulation, we introduce a multi-population Hessian–Riemannian flow algorithm. Furthermore, we prove the global convergence of the proposed algorithm. Unlike projection-based methods, the proposed HRF dynamics preserve the equality constraints by construction. Under the monotonicity and regularity assumptions stated below, the continuous-time flow converges globally to the Wardrop equilibrium. The numerical results show that the method is competitive with standard benchmark solvers and particularly effective in the heterogeneous and emissions-based examples.

The major contributions of this paper are as follows:

- We formulate the multi-population Wardrop *user equilibrium* on generalized directed graphs in edge-flow variables as a variational inequality and establish existence and uniqueness conditions under continuity and (strict) monotonicity assumptions.
- We show that the multi-population Wardrop equilibrium is equivalent to a population-wise Nash equilibrium formulation.
- We propose a distributed Hessian–Riemannian-flow-based method for computing the multi-population Wardrop equilibrium on directed graphs with Kirchhoff flow-conservation constraints. The proposed method is designed to preserve this network structure naturally.
- We prove the global convergence of the proposed method and demonstrate its performance for heterogeneous traffic examples, including an emissions-related scenario, through quantitative comparisons with benchmark approaches such as nonlinear programming, projected gradient, and Gauss–Seidel methods.

The remainder of the paper is organized as follows: in Section 2, we review the equilibrium notions. In Section 3, we introduce the edge-flow Wardrop formulation. In Section 4, we prove well-posedness and the Nash reformulation. In Section 5, we develop the Hessian–Riemannian flow and its convergence analysis. In Section 6, we present numerical experiments, and in Section 7, we conclude and outline directions for future work.

2. Equilibrium and optimality notions

In this section, we clarify the equilibrium and optimality concepts used throughout the paper and fix terminology across the traffic-assignment and game-theoretic viewpoints. We work with *edge-flow* (link-flow) variables and formulate equilibria as *variational inequalities* (VIs), following standard treatments in traffic assignment and network equilibrium [3, 11, 18, 22, 23, 27].

Wardrop I (user equilibrium). Wardrop's first principle models decentralized route choice: At equilibrium, no infinitesimal traveler can reduce its experienced cost by unilaterally changing its route, given the aggregate congestion produced by all travelers [27]. In a link-flow formulation, this equilibrium condition can be expressed as a VI over a feasible set of nonnegative flows satisfying conservation constraints. In particular, equilibrium is characterized by the fact that all feasible deviations fail to decrease the experienced cost induced by the current flow, as formalized in Section 3 using the cost mapping and the feasible set.

Wardrop II (system optimum). Wardrop's second principle corresponds to a centralized system optimum, in which a planner minimizes a global objective such as total travel time. Here, we do not study Wardrop II; we mention it only to distinguish centralized optimization from the decentralized user-equilibrium model studied below.

Multi-population (multi-class) Wardrop I. In multi-population models, travelers are partitioned into classes (populations) with potentially different cost structures, demand profiles, and admissible entry/exit sets. Each population chooses a feasible link-flow vector, while experienced costs are coupled through aggregate congestion, typically depending on the total flow across links. The multi-population Wardrop-I equilibrium is therefore a *coupled* VI: Each population is at equilibrium given the others, and no population can reduce its experienced cost by deviating within its feasible set. This coupling is the main source of analytical and algorithmic complexity in heterogeneous settings and motivates population-wise formulations used later for distributed computation.

Multi-population Wardrop II. The multi-population system-optimal problem assigns flows for all populations to minimize a single global objective that may include class-dependent weights and externalities (e.g., emissions or priority classes), subject to feasibility for each population and any shared constraints [3, 8]. This remains a centralized optimization model and should not be conflated with the user-equilibrium concept of Wardrop I.

Nash viewpoint and its link to multi-population Wardrop I. The multi-population Wardrop-I equilibrium admits a natural game-theoretic interpretation. Each population can be viewed as an aggregate player representing a non-atomic class of travelers: The strategy of population r is its feasible link-flow f^r, and the cost depends on the aggregate flow formed by all populations. Under this interpretation, a multi-population Wardrop-I equilibrium is a Nash equilibrium of the induced population game. Importantly, the VI formulation does *not* require the equilibrium to be the minimizer of a single global objective; such an optimization equivalence generally holds only under additional potential-structure assumptions (which we do not impose in this paper). This distinction is central for the algorithmic perspective developed later. The precise equivalence between the product-space VI and the population-wise Nash conditions is proved in Theorem 5. **Scope used in this paper.** We focus on the multi-population Wardrop *user equilibrium* (Wardrop I) in *edge-flow* variables and use the VI framework as the unifying formulation [11, 22, 23]. All subsequent theoretical and algorithmic results therefore target the Wardrop-I equilibrium and its population-wise coupled formulation, which supports distributed computation and motivates the Hessian–Riemannian-flow dynamics developed in Section 5.

We now make these notions precise in the edge-flow setting.

3. Preliminaries

In this section, we introduce the basic network-flow setting and the major notions that will be used throughout the paper. We begin with the single-population Wardrop model in edge-flow variables and then extend the formulation to the multi-population case.

3.1. Single-population Wardrop model

Following [4, 22], we present the single-population (single-class) network model and the corresponding Wardrop equilibrium in edge-flow variables.

Let $G = (V, E)$ be a directed graph with $|V| = m$ vertices and $|E| = n$ edges. Each edge $e_k \in E$ is an ordered pair $e_k = (v_{s(k)}, v_{t(k)})$ indicating its tail and head. The (nonnegative) link-flow on edge e_k is denoted by $f_k \geq 0$, and we collect all link flows in the vector $f = (f_1, \ldots, f_n)^\top \in \mathbb{R}^n_{\geq 0}$.

Agents enter the network through a set of entrance vertices and exit through a set of exit vertices. Let $V_{\text{out}} \subset V$ denote the set of exit vertices, with $|V_{\text{out}}| = \mu$. We enforce flow conservation on the remaining vertices $V \setminus V_{\text{out}}$, whose cardinality is $m - \mu$.

Define the (reduced) Kirchhoff matrix $K \in \mathbb{R}^{(m-\mu)\times n}$ by

$$K_{i,k} = \begin{cases} 1, & \text{if } e_k \text{ leaves vertex } v_i, \\ -1, & \text{if } e_k \text{ enters vertex } v_i, \\ 0, & \text{otherwise,} \end{cases} \tag{3.1}$$

where i ranges over the non-exit vertices (after any fixed ordering of $V \setminus V_{\text{out}}$). Let $B \in \mathbb{R}^{m-\mu}$ be the net inflow vector under the sign convention of (3.1): Positive entries correspond to net injection that must leave the vertex through outgoing edges. The flow-balance constraints are

$$K\jmath = B. \tag{3.2}$$

We call a link-flow $\jmath$ *admissible* if it satisfies (3.2) and $\jmath \geq \mathbf{0}$. The feasible set is

$$A := \{\jmath \in \mathbb{R}^n : \ \jmath \geq \mathbf{0}, \ K\jmath = B\}. \tag{3.3}$$

Each edge e_k has an associated (possibly flow-dependent) cost $c_k(\jmath)$, and we define the cost mapping

$$c(\jmath) := (c_1(\jmath), \ldots, c_n(\jmath))^\top \in \mathbb{R}^n.$$

The aggregate cost induced by a link flow $\jmath$ is represented by the pairing

$$\langle c(\jmath), \jmath \rangle := \sum_{k=1}^{n} c_k(\jmath)\, \jmath_k.$$

The following remark connects the present edge-flow model with the classical *path-flow* Wardrop formulation. The VI formulation used later requires only a well-defined edge-flow cost operator.

Remark 3.1 (Path-flow versus edge-flow formulations)**.** *Let $\mathcal{P}$ denote a set of admissible directed paths and let $h = (h_p)_{p\in\mathcal{P}}$ be a nonnegative path-flow vector. Define the edge-path incidence matrix $R \in \{0,1\}^{n\times|\mathcal{P}|}$ by*

$$R_{k,p} = \begin{cases} 1, & \text{if edge } e_k \text{ belongs to path } p, \\ 0, & \text{otherwise.} \end{cases}$$

The corresponding edge flows are obtained by aggregation:

$$\jmath = Rh, \qquad \jmath_k = \sum_{p\in\mathcal{P}} R_{k,p}\, h_p.$$

Under additive edge costs, the cost of a path p induced by $c(\jmath)$ is

$$\ell_p(\jmath) = \sum_{k:\, e_k\in p} c_k(\jmath) = \big(R^\top c(\jmath)\big)_p.$$

Working directly with h typically requires enumerating paths in $\mathcal{P}$, which can be prohibitive for large graphs. In contrast, the edge-flow formulation avoids path enumeration and enforces feasibility through the local conservation constraints (3.2)*, which is the viewpoint adopted in this paper.*

We are now ready to introduce the definition of Wardrop equilibrium and the notion of monotonicity, which play central roles in the uniqueness and convergence results established later in the paper.

Definition 1. *A feasible flow $\jmath^* \in A$ is a* Wardrop equilibrium *if, for all $\jmath \in A$,*

$$\langle c(\jmath^*), \jmath^* - \jmath \rangle \leq 0. \tag{3.4}$$

Equivalently, $\jmath^*$ solves the variational inequality VI(A, c)*:*

$$\langle c(\jmath^*), \jmath - \jmath^* \rangle \geq 0, \qquad \forall \jmath \in A.$$

Definition 2. *The mapping $c(\jmath)$ is* monotone *on A if, for all $\jmath_1, \jmath_2 \in A$,*

$$\langle c(\jmath_1) - c(\jmath_2), \jmath_1 - \jmath_2 \rangle \geq 0. \tag{3.5}$$

If the inequality is strict whenever $\jmath_1 \neq \jmath_2$, then c is strictly monotone *on A.*

3.2. Multi-population Wardrop model

In this part, we define the multi-population Wardrop user-equilibrium model in edge-flow variables.

We consider the same directed graph $G = (V, E)$ introduced in Section 3, with the same set of exit vertices (of cardinality μ) and the corresponding reduced Kirchhoff matrix $K \in \mathbb{R}^{(m-\mu)\times n}$. The total population of agents is partitioned into P sub-populations (classes), denoted by $\Lambda_1, \ldots, \Lambda_P$.

Population-wise flows and feasibility. For each population Λ_r, where $r \in \{1, \ldots, P\}$, let

$$\jmath^r := (\jmath^r_1, \ldots, \jmath^r_n)^\top \in \mathbb{R}^n_{\geq 0}$$

denote its edge-flow vector, where $\jmath^r_k$ is the flow of population r on edge e_k. The net input vector for population r is denoted by $B^r \in \mathbb{R}^{m-\mu}$, and feasibility is enforced by the conservation constraints

$$K\jmath^r = B^r, \qquad r = 1, \ldots, P.$$

We collect the population flows in the matrix

$$J := (\jmath^1 \mid \cdots \mid \jmath^P) \in \mathbb{R}^{n\times P}, \qquad \boldsymbol{B} := (B^1 \mid \cdots \mid B^P) \in \mathbb{R}^{(m-\mu)\times P}.$$

Then the coupled flow-balance constraints can be written compactly as

$$KJ = \boldsymbol{B}. \tag{3.6}$$

The admissible set of current distributions for population Λ_r is

$$\mathcal{A}^r := \{\jmath^r \in \mathbb{R}^n_{\geq 0} : K\jmath^r = B^r\},$$

and the admissible set for the entire system is the Cartesian product

$$\boldsymbol{\mathcal{A}} := \mathcal{A}^1 \times \cdots \times \mathcal{A}^P.$$

Hence, J is admissible, that is $J \in \boldsymbol{\mathcal{A}}$, if and only if it satisfies (3.6) and $\jmath^r \geq \mathbf{0}$ for each r.

Population-wise costs and coupling. Each population may have a distinct cost on each edge, and costs may depend on the flows of all populations through congestion effects. For each population r, define its cost vector

$$c^r(J) := \big(c^r_1(J), \ldots, c^r_n(J)\big)^\top \in \mathbb{R}^n,$$

where $c^r_k(J)$ is the cost per unit flow experienced by population r on edge e_k under the full flow profile J. We compile the system operator as the block mapping

$$C(J) := (c^1(J) \mid \cdots \mid c^P(J)) \in \mathbb{R}^{n\times P}.$$

Throughout, when pairing two matrices in $\mathbb{R}^{n\times P}$, we use the Frobenius inner product. In particular, the aggregate experienced cost is

$$\langle C(J), J\rangle := \sum_{r=1}^{P} \langle c^r(J), \jmath^r\rangle = \sum_{r=1}^{P}\sum_{k=1}^{n} \jmath^r_k\, c^r_k(J). \tag{3.7}$$

This quantity is used only as a compact summary of total experienced cost. In general, the Wardrop-I equilibrium below is defined by a VI condition and need not coincide with the minimizer of a single global objective unless additional potential-structure assumptions hold.

Following the previous section, we now present the definition of population-wise Wardrop equilibrium and the corresponding notion of population-wise monotonicity.

Definition 3. *We say that $\bar{J} \in \mathcal{A}$ is a Wardrop equilibrium of the multi-population system if for all $J \in \mathcal{A}$,*

$$\left\langle C(\bar{J}), \bar{J} - J \right\rangle \leq 0. \tag{3.8}$$

Equivalently, $\bar{J}$ solves the variational inequality VI($\mathcal{A}, C$)*:*

$$\left\langle C(\bar{J}), J - \bar{J} \right\rangle \geq 0, \qquad \forall J \in \mathcal{A}.$$

Monotonicity of the operator is the key condition for uniqueness.

Definition 4. *The cost operator $C(J)$ is* monotone *on $\mathcal{A}$ if for all $J_1, J_2 \in \mathcal{A}$,*

$$\langle C(J_1) - C(J_2),\ J_1 - J_2 \rangle \geq 0. \tag{3.9}$$

If the inequality is strict whenever $J_1 \neq J_2$, then C is strictly monotone *on $\mathcal{A}$.*

Population-wise problem. In the multi-population case, we may also consider a Nash equilibrium formulation, which we introduce next and later use in the development of our numerical method. The aggregate cost experienced by population r at the flow profile J is

$$\langle c^r(J), j^r \rangle := \sum_{k=1}^{n} j_k^r c_k^r(J). \tag{3.10}$$

This expression has the same form as in the single-population model, except that the population-r cost may depend on the full profile J, not only on j^r. Now, using this notation, we define the population-wise problem, which is the Nash equilibrium between the populations with coupled population-dependent cost functions.

Definition 5. *A flow profile $J^* = (j^{1*}, \ldots, j^P) \in \mathcal{A}$ is a population-wise* Nash equilibrium *if, for every $r = 1, \ldots, P$,*

$$\langle c^r(J^*), j^{r*} - j^r \rangle \leq 0, \qquad \forall j^r \in \mathcal{A}^r.$$

4. Well-posedness and Nash reformulation

In this section, we collect the major well-posedness results for the single- and multi-population Wardrop models. We first state existence and uniqueness results for the corresponding variational inequalities. We then show that, in the multi-population setting, the Wardrop equilibrium admits an equivalent population-wise Nash reformulation, which will serve as the basis for the numerical method developed in the next section.

4.1. Single-population setting

The existence of solutions to VI(A, c) is a classical result in variational inequality theory; see, for example, [11, Theorem 3.1].

Theorem 1. *Assume that A is nonempty, convex, and compact, and that $c : A \to \mathbb{R}^n$ is continuous. Then, there exists a Wardrop equilibrium.*

Strict monotonicity (see Definition 2) is a standard sufficient condition for uniqueness (see [11, 27]).

Theorem 2. *Assume that c is strictly monotone (see Definition 2) on A. Then,* VI(A, c) *has at most one solution. In particular, under the assumptions of Theorem 1, the Wardrop equilibrium is unique.*

Proof. Suppose $f^{(1)}$ and $f^{(2)}$ are Wardrop equilibria. By (3.4) applied at $f^{(1)}$ with $g = f^{(2)}$ and at $f^{(2)}$ with $g = f^{(1)}$, we have

$$\langle c(f^{(1)}), f^{(1)} - f^{(2)} \rangle \leq 0, \qquad \langle c(f^{(2)}), f^{(2)} - f^{(1)} \rangle \leq 0.$$

Adding yields $\langle c(f^{(1)}) - c(f^{(2)}), f^{(1)} - f^{(2)} \rangle \leq 0$. Strict monotonicity implies $f^{(1)} = f^{(2)}$. □

Remark 4.1. *The strict monotonicity assumption in Theorem 2 (and similarly in the multi-population setting) may be weakened to strict pseudomonotonicity for the purpose of uniqueness. We retain strict monotonicity in this paper to keep the presentation simple and to maintain consistency with the assumptions used later in the convergence analysis of the proposed solver.*

4.2. Multi-population setting and Nash reformulation

We now turn to the multi-population model. We first state the corresponding existence and uniqueness results for the multi-population Wardrop equilibrium, and then show that this problem is equivalent to a population-wise Nash formulation.

Similar to the single-population case, the existence result follows from [11, Theorem 3.1].

Theorem 3. *Assume that $\mathcal{A}$ is nonempty, convex, and compact, and that $C : \mathcal{A} \to \mathbb{R}^{n \times P}$ is continuous. Then, there exists a Wardrop equilibrium.*

Strict monotonicity guarantees uniqueness whenever a solution exists.

Theorem 4. *Assume that $C(\cdot)$ is strictly monotone (see Definition 4) on $\mathcal{A}$. Then, there is at most one Wardrop equilibrium.*

Proof. Assume J_1 and J_2 are both Wardrop equilibria. Applying (3.8) at J_1 with $J = J_2$ and at J_2 with $J = J_1$ yields

$$\langle C(J_1), J_1 - J_2 \rangle \leq 0, \qquad \langle C(J_2), J_2 - J_1 \rangle \leq 0.$$

Adding gives $\langle C(J_1) - C(J_2), J_1 - J_2 \rangle \leq 0$. Strict monotonicity implies $J_1 = J_2$. □

In the previous section, we defined a coordinate-wise solution or Nash equlibiram (see Definition 5). Because the feasible set is a Cartesian product, the multi-population Wardrop VI is equivalent to the population-wise Nash conditions. This equivalence does not require monotonicity.

Theorem 5. *Let $\mathcal{A} = \mathcal{A}^1 \times \cdots \times \mathcal{A}^P$. A flow profile $\bar{J} \in \mathcal{A}$ solves the multi-population Wardrop VI* (3.8) *if and only if it satisfies the population-wise Nash conditions* (3.10)*. That is, The population-wise (Nash) and Wardrop problems are equivalent.*

Proof. We prove that Wardrop equilibrium is a population-wise solution.

Let $\bar{J} \in \mathcal{A}$ be a Wardrop equilibrium; that is, (3.8) holds for $\bar{J} \in \mathcal{A}$ and any $J \in \mathcal{A}$. Now, in (3.8) taking $j^i = \bar{j}^i$ for all $i \in \{1, 2, \ldots, P\}$ and $i \neq r$ by (3.7), we get

$$\left\langle c^r(\bar{J}), \bar{j}^r - j^r \right\rangle \leq 0.$$

Hence, $\bar{J}$ is a population-wise solution.

Conversely, every population-wise Nash solution is a Wardrop equilibrium.

Suppose $J^* \in \mathcal{A}$ is a population-wise solution. Then, adding up (3.10) for all $r = 1, \ldots, P$, we obtain (3.8). □

5. Main approach

Using population-wise formulation, we propose a numerical solver based on Hessian-Riemannian flow (HRF) [2]. Unlike classical Euclidean methods, HRF naturally respects boundaries and constraints through the metric; no need for external projection steps. Furthermore, the method is globally convergent, and we adapt to find Wardrop equilibrium.

In [2], the authors proposed a method for solving a minimization problem under equality constraint in a convex and open set. It consists of endowing the open convex set with a Riemannian structure, which restricts the search to the relative interior of the feasible set defined by the linear equality. By applying the Hessian steepest descent method, orthogonally projected onto the Riemannian manifold, one obtains a projected gradient descent solution for the constrained problem. In this formulation, the steepest descent method becomes a local minimization process on a Riemannian manifold, where a vector field generates solution trajectories based on initial conditions from the interior of the domain. The approach in [2] is called the Hessian-Riemannian gradient flow (HRGF), which is constructed using the cost function gradient. In [9], in the context of mean-field games, the authors demonstrated that the gradient of the cost function in the HRGF approach can be replaced with monotone operators. Motivated by this, we use Hessian-Riemannian flow to solve the system of variational inequalities defined by the multi-population Wardrop equilibrium.

We start by considering the single population problem in (3.10) with fixed $J_F^{-r} := (J_F^1, \dots, J_F^{r-1}, J_F^{r+1}, \dots, J_F^P) \in \mathbb{R}^{n\times(P-1)}$ and aim to find $\vec{\jmath}^r \in \mathcal{A}^r$ such that for all $\jmath^r \in \mathcal{A}^r$ the following inequality holds

$$\langle c^r(\vec{\jmath}^r, J_F^{-r}), \vec{\jmath}^r - \jmath^r)\rangle \leq 0. \tag{5.1}$$

Remark 5.1. *In some cases, the population r may occupy some part of the original graph G. Particularly, if there are total λ_T entry vertices, the r population agents enter the network only when $\lambda_r < \lambda_T$. In this case, the r-th population's current on the remaining $(\lambda_T - \lambda_r)$ entry vertices is* 0.

To initiate the HRF method, we require an interior point, $\jmath^r > 0$. Hence, if the r-th population always has zero current on some edge, we cannot properly initialize the HRF. Therefore, if it is known *a priori* that the r-th population always has zero current on certain λ_{-r} edges, we remove those edges from the original graph. This results in a subgraph G_r, along with the corresponding (full rank) Kirchhoff matrix K_r and B_R^r, which corresponds to a non-exit vertex. This process does not affect the solution and ensures that we can select an interior point required to initialize the HRF.

Now, relying on the discussion above, we reformulate the problem in (5.1). Thus, instead of an original distribution of currents $\jmath^r \in \mathbb{R}^n$, we consider its sub-vector $\vartheta^r \in \mathbb{R}^{n-\lambda_{-r}}$ (all constant 0 components are removed). The admissible set for each population becomes $\mathcal{A}_R^r := \{\vartheta^r \in \mathbb{R}^{n-\lambda_{-r}} : \vartheta^r \geq 0,\ K_r\vartheta^r = B_R^r\}$ and for the population, we set $\boldsymbol{\mathcal{A}}_R := \mathcal{A}_R^1 \times \cdots \times \mathcal{A}_R^P$. Thus, the population-wise problem reads as follows:

Problem 5.1. *For fixed $\boldsymbol{\vartheta}^{-r} := (\vartheta^1, \dots, \vartheta^{r-1}, \vartheta^{r+1}, \dots, \vartheta^P) \in \prod_{i=1, i\neq r}^P \mathcal{A}_R^i$ find $\bar{\vartheta}^r \in \mathcal{A}_R^r$ such that for all $\vartheta^r \in \mathcal{A}_R^r$, the following inequality holds*

$$\left\langle c^r(\bar{\vartheta}^r, \boldsymbol{\vartheta}^{-r}), \bar{\vartheta}^r - \vartheta^r\right\rangle \leq 0, \tag{5.2}$$

where we abuse the notation with $c^r(\bar{\vartheta}^r, \boldsymbol{\vartheta}^{-r}) := c^r(\jmath^r, \boldsymbol{\jmath}^{-r})$.

For fixed $\boldsymbol{\vartheta}^{-r} = (\vartheta^1, \ldots, \vartheta^{r-1}, \vartheta^{r+1}, \ldots, \vartheta^P)$, we find a solution to Problem 5.1 by the HRF method, which leads to the solution of an ODE. Therefore, to find a population-wise problem solution for all $\boldsymbol{\vartheta}^{-r} = (\vartheta^1, \ldots, \vartheta^{r-1}, \vartheta^{r+1}, \ldots, \vartheta^P)$, $r = 1, \ldots, P$, we write the corresponding ODE and end up with a coupled system of ODEs, the solution of which, due to the HRF method, converges to the solution of our population-wise problem, later shown to be Wardrop equilibrium.

For our main result, we consider the following:

$$h_r(x) = \sum_{k=1}^{n-\lambda_{-r}} x_k \log x_k,$$

Legendre-type strictly convex function on $\mathbb{R}^{n-\lambda_{-r}}_{\geq 0}$ (see Definition 3.1 in [2]). Let $H_r(x) = \nabla^2 h_r(x)$ and set

$$F_r(\vartheta^r) = \left[I - K_r^T M_r(\vartheta^r)\right], \tag{5.3}$$

where

$$M_r(\vartheta^r) = \left(K_r H_r(\vartheta^r)^{-1} K_r^T\right)^{-1} K_r H_r(\vartheta^r)^{-1}.$$

For the proof, we use the h-divergence (Bregman divergence) function associated with h_r, defined as

$$d_{h_r}(x, y) = h_r(x) - h_r(y) - (x - y) \cdot \nabla h_r(y), \tag{5.4}$$

which is non-negative and strictly positive whenever $x \neq y$.

The following theorem establishes convergence of the continuous-time HRF dynamics. The numerical discretization used in Section 6 is described separately.

Theorem 6. *Assume that each $\mathcal{A}_R^r$ is nonempty, compact, and has nonempty relative interior. Furthermore, assume that the cost functions $c^r(\cdot)$ are continuous, locally Lipchitz and strictly monotone. Suppose that $\boldsymbol{\vartheta}(0) = \boldsymbol{\vartheta}_0 > 0$, such that $\vartheta_0^r \in \mathcal{A}_R^r$, and $\boldsymbol{\vartheta}(t) = (\vartheta^1(t), \ldots, \vartheta^P(t))$ solves the following system of ODEs*

$$\begin{cases} \dot{\vartheta}^r + H_r(\vartheta^r)^{-1} F_r(\vartheta^r) c^r(\vartheta^r, \boldsymbol{\vartheta}^{-r}) = 0, \\ \vartheta^r(0) = \vartheta_0^r, \end{cases} \qquad r = 1, \ldots, P, \tag{5.5}$$

where F_r is defined by (5.3)*. Then, $\vartheta^r(t) \in \mathcal{A}_R^r$ for all $t \geq 0$. Moreover, there exists $\lim_{t\to\infty} \boldsymbol{\vartheta}(t) = \boldsymbol{\vartheta}_\infty$, and J_∞, corresponding to $\boldsymbol{\vartheta}_\infty$, is the Wardrop equilibrium.*

Proof. Note that by Theorem 5, it is enough to prove that there exists $\lim_{t\to\infty} \boldsymbol{\vartheta}(t) = \boldsymbol{\vartheta}_\infty \in \mathcal{A}_R$, then, the corresponding $\boldsymbol{J}_\infty \in \mathcal{A}$ solves Problem 5.1.

We first prove the well-posedness of (5.5). The theorem assumptions with the definition of H_r imply that the right-hand side of (5.5) is locally Lipschitz in $\boldsymbol{\vartheta}$. Therefore, by the Picard–Lindelöf theorem, solutions' local existence and uniqueness follow.

Next, we prove the global existence and uniqueness of the solutions. Let $\{\vartheta^r(t)\}_{r=1}^P$ be a solution to (5.5). Note that

$$K_r H_r(\vartheta^r)^{-1} F_r(\vartheta^r) = K_r H_r(\vartheta^r)^{-1} - K_r H_r(\vartheta^r)^{-1} K_r^T (K_r H_r(\vartheta^r)^{-1} K_r^T)^{-1} K_r H_r(\vartheta^r)^{-1} = 0,$$

which, along with (5.5), implies that $K_r\dot{\vartheta}^r(t) = 0$. Using this and recalling that $K_r\vartheta^r(0) = K_r\vartheta_0^r = B^r$, we get

$$K_r\vartheta^r(t) = \int_0^t K_r\dot{\vartheta}^r(s)ds + K_r\vartheta^r(0) = K_r\vartheta_0^r = B^r. \tag{5.6}$$

By Theorems 3–5, it follows that Problem 5.1 admits a unique solution. Let $\bar{\boldsymbol{\vartheta}} \in \mathcal{A}_R$ be the unique solution to Problem 5.1. Hence, by (5.6), we have

$$\left(\bar{\vartheta}^r - \vartheta^r(t)\right)^T K_r^T = 0. \tag{5.7}$$

Because c^r is strictly monotone and $\bar{\vartheta}$ is the solution to Problem 5.1, by combining (3.9) and (5.2), we obtain

$$\left\langle c^r(\boldsymbol{\vartheta}), \vartheta^r - \bar{\vartheta}^r \right\rangle = \left\langle c^r\left(\bar{\vartheta}^r, \boldsymbol{\vartheta}^{-r}\right) - c^r\left(\vartheta^r, \boldsymbol{\vartheta}^{-r}\right), \bar{\vartheta}^r - \vartheta^r \right\rangle - \left\langle c^r\left(\bar{\vartheta}^r, \boldsymbol{\vartheta}^{-r}\right), \bar{\vartheta}^r - \vartheta^r \right\rangle > 0.$$

Taking $\boldsymbol{\vartheta} = \boldsymbol{\vartheta}(t)$ in the proceeding equation, we get

$$\left\langle c^r(\boldsymbol{\vartheta}(t)), \bar{\vartheta}^r - \vartheta^r(t) \right\rangle = \left(\bar{\vartheta}^r - \vartheta^r(t)\right)^T c^r(\boldsymbol{\vartheta}(t)) < 0. \tag{5.8}$$

Recalling that h^r is strictly convex function for $\bar{\vartheta}^r \neq \vartheta^r(t)$, we have

$$\begin{aligned} d_{h_r}(\bar{\vartheta}^r, \vartheta^r(t)) &= h_r(\bar{\vartheta}^r) - h_r(\vartheta^r(t)) - (\bar{\vartheta}^r - \vartheta^r(t))^T \nabla h_r(\vartheta^r(t)) \\ &= h_r(\bar{\vartheta}^r) - (\bar{\vartheta}^r)^T \log \vartheta^r(t) + \vartheta^r(t) - \bar{\vartheta}^r > 0. \end{aligned} \tag{5.9}$$

Next, we show that $d_{h_r}(\bar{\vartheta}^r, \vartheta^r(t))$ strictly decreases. To do so, we consider the time derivative of $d_{h_r}(\bar{\vartheta}^r, \vartheta^r(t))$

$$\begin{aligned} \frac{d}{dt} d_{h_r}(\bar{\vartheta}^r, \vartheta^r(t)) &= -\dot{\vartheta}^{r^T}(t)\nabla h_r(\vartheta^r(t)) + \dot{\vartheta}^{r^T}(t)\nabla h_r(\vartheta^r(t)) - \left(\bar{\vartheta}^r - \vartheta^r(t)\right)^T H_r(\vartheta^r(t))\dot{\vartheta}^r(t) \\ &= -\left(\bar{\vartheta}^r - \vartheta^r(t)\right)^T H_r(\vartheta^r(t))\dot{\vartheta}^r(t). \end{aligned}$$

Using expression of $\dot{\vartheta}^r(t)$ from (5.5) in the proceeding equation, by equations in (5.7) and (5.3), we get

$$\begin{aligned} \frac{d}{dt} d_{h_r}(\bar{\vartheta}^r, \vartheta^r(t)) &= \left(\bar{\vartheta}^r - \vartheta^r(t)\right)^T c^r(\boldsymbol{\vartheta}(t)) + \left(\bar{\vartheta}^r - \vartheta^r(t)\right)^T K_r^T M_r(\vartheta^r(t)) c^r(\boldsymbol{\vartheta}(t)) \\ &= \left(\bar{\vartheta}^r - \vartheta^r(t)\right)^T c^r(\boldsymbol{\vartheta}(t)) < 0, \end{aligned} \tag{5.10}$$

where the last inequality follows from (5.8). On the other hand, note that for any $a > 0$, there exists $M > 0$, such that

$$|\{d_{h_r}(\vartheta^r, y) \leq a : y \in \mathbb{R}_{>0}^{n-\lambda_{-r}}\}| \leq M.$$

Along with the Eqs (5.9) and (5.10), this implies that $\vartheta^r(t)$ is bounded. Therefore, by Theorem 3.3 in [12], we deduce that for all $t \geq 0$, there exists a unique solution to (5.5), defined as $\{\vartheta^r(t)\}_{r=1}^P$. Furthermore, there exists $\boldsymbol{\vartheta}_\infty \geq 0$, such that $\lim_{t\to\infty} \boldsymbol{\vartheta}(t) = \boldsymbol{\vartheta}_\infty$. Next, we prove that $\boldsymbol{\vartheta}_\infty$ solves Problem 5.1. Note that Eqs (5.9) and (5.10), together with the non-negativity of the function d_{h_r}, imply that $\bar{\vartheta}^r$ is an equilibrium point of Eq (5.5). Furthermore, by the definition of d_{h_r} function, see (5.4), and by (5.10), we deduce that the function $\sum_{r=1}^P d_{h_r}(\bar{\vartheta}^r, \cdot)$ is a Lyapunov function. Therefore, by [12, Theorem 4.2], the solution $\{\vartheta^r(t)\}_{r=1}^P$ is globally convergent to $\bar{\boldsymbol{\vartheta}}$. □

6. Simulation results

In this section, we present three simulation scenarios in which we compare the proposed method with several well-known benchmark approaches. In the first scenario, we validate the proposed multi-population framework by comparing it with nonlinear programming (NLP), projected gradient, and Gauss–Seidel methods. In the second scenario, we examine the effect of heterogeneous multi-population congestion, in particular a setting in which trucks experience twice the congestion cost of cars. In the third scenario, we demonstrate how the multi-population method can be used for traffic management with the objective of reducing overall emissions, and we show that the multi-population HRF method provides the most favorable balance between computational efficiency and solution quality among the methods considered.

6.1. Scenario 1

To validate our approach, we compare a uniform population nonlinear programming solver, a uniform population HRF solver, and a multi-population HRF solver, projected gradient, Gauss–Seidel. All methods yield the same solution. Scenario 1 serves as a baseline synthetic benchmark for validating the proposed method in a standard Wardrop-type setting with linear congestion costs.

We consider a case with two populations having equal weights. In this scenario, the cost on each edge is the flow on that edge for both populations: $c_k(\jmath_k) = \jmath_k^1 + \jmath_k^2$, where $\jmath_k^i$ denotes the flow of population i on edge k. The overall road graph is modeled by the connected graph shown in Figure 1a.

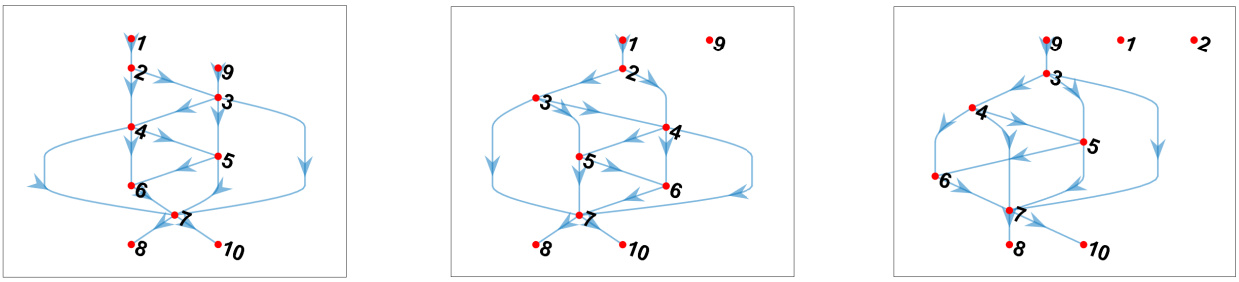

(a) Full road graph representing all roads. **(b)** Population 1 flow sub-graph. **(c)** Population 2 flow sub-graph.

Figure 1. Individual population sub-graphs.

Each population utilizes only a portion of the overall network. In this setting, $\jmath^1$ (population 1) enters exclusively at node 1, while $\jmath^2$ (population 2) enters exclusively at node 9.

6.1.1. Uniform population

Under the uniform population assumption, we aggregate the flows as $\jmath = \jmath^1 + \jmath^2$ and define the cost on edge k as $c_k(\jmath_k) = \jmath_k$. Considering that the inflows at nodes 1 and 9 are both 100, the net input vector for the Kirchhoff equation $K\jmath = B_0$ is given by $B_0 = [100, 0, 0, 0, 0, 0, 0, 100]^T$. Simulating Eq (5.5) for the single-population case yields the equilibrium flow distribution shown in Table 1. Note that the flow values are rounded to the nearest integer.

6.1.2. Nonlinear programming

Alternatively, since the cost function is linear, and therefore the problem can be formulated as a constrained optimization problem, we can solve:

$$\min \ \frac{1}{2}\sum_{i=1}^{15} J_i^2, \quad \text{s.t. } KJ = B_0, \ J_i \geq 0, \quad \forall\, i \in \{1, \ldots, 15\}.$$

The same solution is obtained using a conventional interior-point method. We set the solution of NLP, as a benchmark and compare other methods with its solution.

6.1.3. Multi-population solution

The uniform population approach does not differentiate the flow contributions of each population. For the multi-population solution, each population has its own flow vector and is constrained to its subgraph. Figures 1b and 1c illustrate the subgraphs for each population. The inflows for both populations are 100. Each population satisfies its own Kirchhoff law, and costs are coupled through $c_k(J_k) = J_k^1 + J_k^2$. Because the HRF converges under the assumptions of Theorem 6, we initialize the ODE system (5.5) with an initial guess for J. The system converges to the equilibrium solution and obtains the same results as shown in Table 1.

Table 1. The equilibrium flow distributions for Scenario 1.

Edges	(1,2)	(2,3)	(9,3)	(2,4)	(3,4)	(3,5)	(4,5)	(4,6)	(5,6)	(3,7)	(4,7)	(5,7)	(6,7)	(7,8)	(7,10)
Flow 1	100	38	0	62	1	13	10	15	4	24	39	19	18	50	50
Flow 2	0	0	100	0	23	24	2	7	6	52	13	21	13	50	50
Total Flow	100	38	100	62	24	37	12	22	10	76	54	40	31	100	100

We are now ready to compare the performance of the numerical methods. Table 2 shows that all methods recover the benchmark equilibrium with very high accuracy. As expected, the uniform NLP solver is the fastest method overall, since Scenario 1 reduces to a small convex quadratic program with linear constraints. Among the iterative methods, the uniform HRF and the multi-population HRF achieve essentially machine-precision agreement with the NLP solution, with errors of order 10^{-11} or smaller in ℓ_2 and ℓ_∞. The projected-gradient and Gauss–Seidel methods are also highly accurate, though their errors are larger, at the level of 10^{-7} in ℓ_2 and ℓ_∞. In terms of computational time, projected gradient and Gauss–Seidel are faster than the HRF-based methods in this simple benchmark, while the HRF methods provide the highest numerical accuracy among the iterative schemes.

Table 2. Comparison of numerical methods for Scenario 1. The uniform NLP is used as the benchmark.

Method	Time (s)	Iter./Steps	ℓ_2 dist. to NLP	Max diff. to NLP
Uniform NLP	0.00053	2	0	0
Uniform HRF	0.05210	590	3.52×10^{-12}	1.68×10^{-12}
Multi-population HRF	0.07172	474	1.53×10^{-11}	7.29×10^{-12}
Projected gradient	0.00862	37	2.54×10^{-7}	1.39×10^{-7}
Gauss–Seidel	0.00808	21	6.08×10^{-7}	2.92×10^{-7}

6.2. *Scenario 2*

In this scenario, we consider the same graph as in Scenario 1, but we now account for heterogeneous congestion sensitivity across populations. Scenario 2 is a heterogeneous multi-population benchmark motivated by multi-class traffic assignment models with asymmetric car–truck interactions; see, e.g., [8, 14].

We assume that population 1 corresponds to cars and population 2 corresponds to trucks, where trucks experience twice the congestion cost of cars. The cost function is chosen to be

$$c_k^r(J) = 0.5(J_k^1 + 2J_k^2) + 0.5\, J_k^r.$$

The resulting equilibrium flows for each population are shown in Figure 2a and 2b, respectively.

For this scenario, Table 3 shows that all methods recover essentially the same equilibrium flow profile in the heterogeneous multi-population setting, thereby validating the proposed formulation and solver for genuinely class-dependent costs. The weighted-potential NLP serves as a natural benchmark for this particular affine cost structure. Among the iterative methods, the proposed multi-population HRF exhibits the closest agreement with the NLP solution, with an ℓ_2 distance of order 10^{-8}. The Gauss–Seidel scheme also performs well, achieving an accuracy of order 10^{-7}, although it is slower than HRF in this experiment. By contrast, the projected-gradient method is both significantly slower and less accurate, despite preserving feasibility. Overall, these results indicate that, in the heterogeneous multi-population setting, the proposed HRF method provides the best balance between accuracy and computational efficiency among the iterative schemes considered.

Table 3. Comparison of numerical methods for the heterogeneous multi-population Scenario 2. The weighted-potential NLP is used as the benchmark.

Method	Time (s)	Iter./Steps	ℓ_2 dist. to NLP	Max diff. to NLP
Weighted-potential NLP	0.04848	83	0	0
Multi-population HRF	0.08864	564	4.13×10^{-8}	2.28×10^{-8}
Projected gradient	7.58396	500	2.07×10^{-4}	8.93×10^{-5}
Gauss–Seidel	0.32830	23	2.02×10^{-7}	1.12×10^{-7}

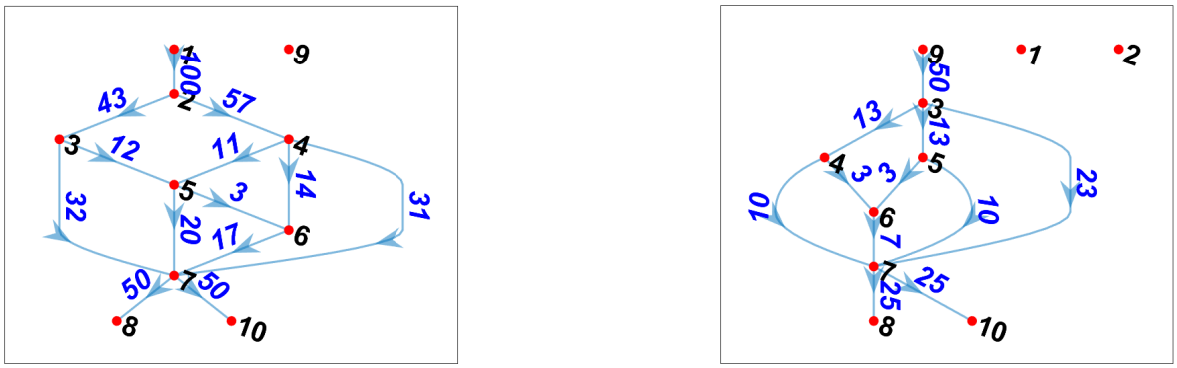

(a) Car flow sub-graph

(b) Truck flow sub-graph

Figure 2. Individual population sub-graphs.

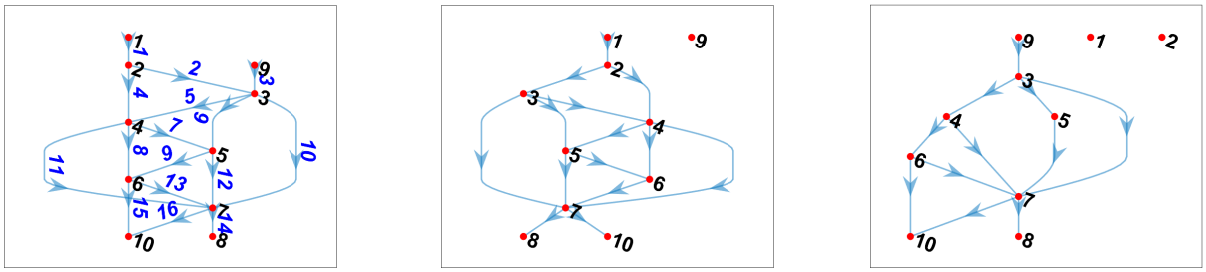

(a) Full road graph with edge length (s_k) **(b)** Car flow sub-graph **(c)** Truck flow sub-graph

Figure 3. Individual population sub-graphs and road lengths.

6.3. Reducing emission cost with traffic management

One major problem in dense urban environments arises from vehicle emissions, which impacts both public health and fuel consumption costs. This scenario is application-driven and follows established emissions and fuel-consumption modeling ideas from the literature; in particular, the cost structure is motivated by [26], from which we adapt Table 4. In [26], models for fuel consumption (FC) and emissions, specifically hydrocarbons (HC), nitrous oxides (NOx), carbon monoxide (CO), and carbon dioxide (CO2), are discussed. Emissions are computed using the average speed of the vehicles on every edge, which is affected by the total flow in the respective edges. The average speed described by the flow on the edge:

$$v_k(J_k) = \frac{s_k}{t_k}\left(1 + \alpha_k \left(\frac{J_k}{\kappa_k}\right)^{\beta_k}\right)^{-1},$$

where $s_k > 0$ is the length of edge k, $t_k > 0$ is the free flow travel time, $\alpha_k > 0$ and $\beta_k > 0$ are congestion parameters, and $\kappa_k > 0$ is the practical capacity. The total flow on the edge is $J_k = \sum_{r=1}^{P} J_k^r$. The emissions are described by the flow on each respective edge by the following equation:

$$e^r_{\{k,j\}}(J_k) = \frac{a^r_j}{v_k(J_k)} + b^r_j.$$

Here, a^r_j and b^r_j are parameters calibrated for each species, with $a^r_j > 0$. The cost function is chosen as:

$$c^r_k(J) = \frac{s_k}{2} \sum_j w_j \, 10^{-3} \, e^r_{\{k,j\}}(J_k) + \frac{j^r_k}{2},$$

where w_j denotes the cost of emission j in $\$/kg$. The values for a^r_j and b^r_j for cars are provided in Table 4. Trucks are assumed to emit three times as much as cars, i.e., $e^2_{\{k,j\}} = 3e^1_{\{k,j\}}$.

Table 4. Parameters for each emission type for standard cars under optimal speed.

Objective (g/km)	a (g/h)	b (g/km)	w (\$/kg)
FC	1.56×10^3	3.54×10^1	1.0321
HC	1.08×10^1	-7.11×10^{-3}	12.91
NOx	2.00×10^0	-4.49×10^{-2}	14.54
CO	8.08×10^1	1.16×10^0	0.37
CO2	4.78×10^3	1.11×10^2	0.02

In the simulation, we set $t_k = \frac{s_k}{50}$, so that free-flow speed satisfies $\frac{t_k}{s_k} = 50$ km/hr for all edges. Moreover, we set $\beta_k = 3$, $\alpha_k = 5$, and $\kappa_k = 50$ for all k. The graph with road lengths is shown in Figure 3a, and the corresponding population subgraphs are shown in Figure 3b,3c.

We simulate the system using the same methods as in the previous scenarios. However, in this case, there is no NLP benchmark solution, so the methods are compared directly against one another. Table 5 shows that the HRF and Gauss–Seidel methods produce very similar solutions, while the projected-gradient method deviates more from the HRF reference profile, although it remains reasonably close. Therefore, we take the HRF solution as the reference solution in this scenario. In particular, the Gauss–Seidel solution differs from HRF only by 4.55×10^{-3} in the ℓ_2 norm and by 2.28×10^{-3} in the ℓ_∞ norm, whereas the projected-gradient method exhibits significantly larger discrepancies. In terms of computational time, the proposed HRF method is the fastest among the three methods considered. In particular, it is approximately twice as fast as Gauss–Seidel and more than one order of magnitude faster than projected gradient, while producing a solution that is nearly indistinguishable from the Gauss–Seidel solution. These results indicate that, HRF provides the best balance between computational efficiency and solution quality in complex scenarios, while Gauss–Seidel remains a competitive alternative.

Table 5. Comparison of numerical methods for the emissions-based multi-population scenario. The HRF solution is used as the reference profile.

Method	Time (s)	Iter./Steps	ℓ_2 dist. to HRF	Max diff. to HRF
Multi-population HRF	6.9011	24975	0	0
Projected gradient	150.1421	8000	1.0612	4.7196×10^{-1}
Gauss–Seidel	13.3662	900	4.55×10^{-3}	2.28×10^{-3}

The corresponding flow distributions are shown in Figure 4a,4b. They indicate that the resulting equilibrium not only reduces the emissions-related component of the cost, but also reduces congestion by distributing the flow in a balanced way across the network.

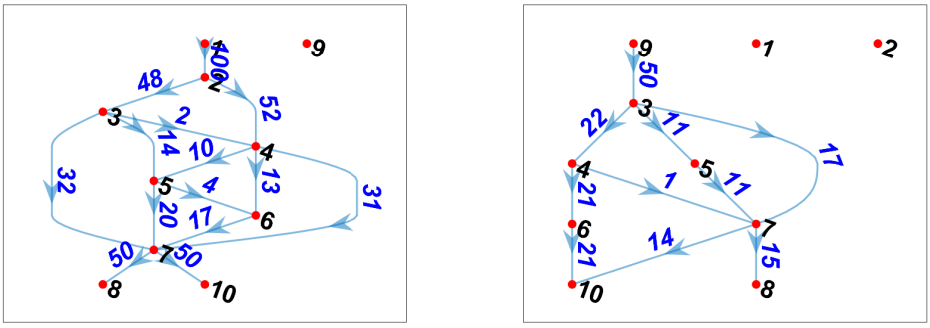

(a) Minimum emission car population. **(b)** Minimum emission truck population.

Figure 4. Minimum emission individual populations.

7. Conclusions

In this paper, we developed an analysis and a numerical method for the multi-population Wardrop user equilibrium problem. We formulated the single- and multi-population settings in edge-flow variables and expressed the equilibrium conditions as a variational inequality over a feasible set defined by conservation (Kirchhoff) equalities and nonnegativity constraints. Under standard continuity and (strict) monotonicity assumptions, we provided existence and uniqueness conditions for the multi-population Wardrop equilibrium and related the centralized Wardrop VI to a population-wise coupled VI formulation, which admits a Nash-equilibrium interpretation for interacting populations. We then proposed distributed Hessian–Riemannian-flow dynamics for solving the resulting coupled VI: Each population evolves its own edge flows, while coupling appears through the congestion-dependent costs. We showed that, under appropriate conditions, the induced continuous-time dynamics converge to the unique multi-population Wardrop equilibrium. Finally, we illustrated the approach through three simulation scenarios. In the emissions-based example, HRF reaches the reference profile faster than the projected-gradient and Gauss–Seidel implementations used in our experiments. In future work, we will consider discrete-time and asynchronous implementations, extensions to time-varying demands, and additional network constraints.

Author contributions

Tigran Bakaryan and Christoph Aoun have contributed through **Conceptualization**, **Investigation**, and **Methodology**, including **Formal analysis**, **Validation**, **Software**, and **Visualization**. They are also responsible for **Writing – original draft** and subsequent **Writing – review & editing**.

Ricardo de Lima Ribeiro, Naira Hovakimyan, and Diogo Gomes supported the research through **Supervision**, **Project administration**, and **Resources**, including **Writing – review & editing** of the journal drafts. All authors have read and approved the final version of the manuscript for publication.

Use of Generative-AI tools declaration

The authors declare that Artificial Intelligence (AI) tools were used in the preparation of this article solely for English language editing and proofreading of the final manuscript.

Acknowledgments

The work of TB was supported by the Higher Education and Science Committee of MESCS RA, Research Project, 24IRF-1A001. The work of CA and NH was supported by National Aeronautics and Space Administration (NASA) University Leadership Initiative (ULI) grant 80NSSC17M0051.

Conflict of interest

All authors declare no conflicts of interest in this paper.

References

1. E. Altman, T. Basar, T. Jimenez, N. Shimkin, Competitive routing in networks with polynomial cost, *Proceedings IEEE INFOCOM 2000. Conference on Computer Communications. Nineteenth Annual Joint Conference of the IEEE Computer and Communications Societies*, Tel Aviv, Israel: IEEE, **3** (2000), 1586–1593. https://doi.org/10.1109/infcom.2000.832557
2. F. Alvarez, J. Bolte, O. Brahic, Hessian riemannian gradient flows in convex programming, *SIAM J. Control Optim.*, **43** (2004), 477–501. https://doi.org/10.1137/s0363012902419977
3. M. J. Beckmann, C. B. McGuire, C. B. Winsten, *Studies in the economics of transportation*, Santa Monica, CA: RAND Corporation, 1955.
4. F. Al Saleh, T. Bakaryan, D. Gomes, R. de Lima Ribeiro, First-order mean-field games on networks and wardrop equilibrium, *Port. Math.*, **81** (2024), 201–246. https://doi.org/10.4171/pm/2124
5. U. Bhaskar, L. Fleischer, D. Hoy, C. C. Huang, Equilibria of atomic flow games are not unique, *Proceedings of the Twentieth Annual ACM-SIAM Symposium on Discrete Algorithms (SODA)*, SIAM, 2009, 748–757. https://doi.org/10.1137/1.9781611973068.82
6. J. R. Correa, N. E. Stier-Moses, Wardrop equilibria, In: *Wiley encyclopedia of operations research and management science*, John Wiley & Sons, Ltd., 2011. https://doi.org/10.1002/9780470400531.eorms0962
7. F. Facchinei, C. Kanzow, Generalized nash equilibrium problems, *Ann. Oper. Res.*, **175** (2010), 177–211. https://doi.org/10.1007/s10479-009-0653-x
8. M. Gairing, M. Klimm, Congestion games with player-specific costs revisited, In: B. V"ocking, *Algorithmic game theory*, SAGT 2013, Lecture Notes in Computer Science, Berlin, Heidelberg: Springer, 2013, 98–109. https://doi.org/10.1007/978-3-642-41392-6_9
9. D. A. Gomes, X. Yang, The hessian riemannian flow and newton's method for effective hamiltonians and mather measures, *ESAIM: Math. Model. Numer. Anal.*, **54** (2020), 1883–1915.
10. A. Haurie, P. Marcotte, On the relationship between nash–cournot and wardrop equilibria, *Networks*, **15** (1985), 295–308. https://doi.org/10.1002/net.3230150303
11. P. T. Harker, J. S. Pang, Finite-dimensional variational inequality and nonlinear complementarity problems: a survey of theory, algorithms and applications, *Math. Program.*, **48** (1990), 161–220. https://doi.org/10.1007/bf01582255
12. H. K. Khalil, *Nonlinear systems*, 3 Eds., Upper Saddle River, NJ: Prentice Hall, 2002.
13. Y. Li, W. Jia, L. Liu, Cooperative emergence induced by asymmetric punishment and strategy persistence mechanisms in multilayer networks, *Commun. Nonlinear Sci. Numer. Simul.*, **152** (2026), 109187. https://doi.org/10.1016/j.cnsns.2025.109187
14. H. S. Mahmassani, K. C. Mouskos, Some numerical results on the diagonalization algorithm for network assignment with asymmetric interactions between cars and trucks, *Transp. Res. Part B: Methodol.*, **22** (1988), 275–290. https://doi.org/10.1016/0191-2615(88)90004-5
15. F. Meunier, T. Pradeau, A lemke-like algorithm for the multiclass network equilibrium problem, In: Y. Chen, N. Immorlica, *Web and internet economics*, Berlin, Heidelberg: Springer, 2013, 363–376. https://doi.org/10.1007/978-3-642-45046-4_30

16. F. Meunier, T. Pradeau, Computing solutions of the multiclass network equilibrium problem with affine cost functions, *Ann. Oper. Res.*, **274** (2019), 447–469. https://doi.org/10.1007/s10479-018-2817-z

17. A. Orda, R. Rom, N. Shimkin, Competitive routing in multi-user communication networks. *Proceedings of IEEE INFOCOM '93: The Conference on Computer Communications*, Vol. 3, San Francisco, CA, USA: IEEE, 1993, 964–971. https://doi.org/10.1109/infcom.1993.253270

18. M. Patriksson, *The traffic assignment problem: models and methods*, Dover Publications, 2015.

19. D. Paccagnan, B. Gentile, F. Parise, M. Kamgarpour, J. Lygeros, Nash and wardrop equilibria in aggregative games with coupling constraints, *IEEE Trans. Automat. Control*, **64** (2019), 1373–1388. https://doi.org/10.1109/tac.2018.2849946

20. O. Richman, N. Shimkin, Topological uniqueness of the nash equilibrium for selfish routing with atomic users, *Math. Oper. Res.*, **32** (2007), 215–232. https://doi.org/10.1287/moor.1060.0229

21. J. B. Rosen, Existence and uniqueness of equilibrium points for concave n-person games, *Econometrica*, **33** (1965), 520–534. https://doi.org/10.2307/1911749

22. M. J. Smith, The existence, uniqueness and stability of traffic equilibria, *Transp. Res. Part B: Methodol.*, **13** (1979), 295–304. https://doi.org/10.1016/0191-2615(79)90022-5

23. M. J. Smith, Junction interactions and monotonicity in traffic assignment, *Transp. Res. Part B: Methodol.*, **16** (1982), 1–3. https://doi.org/10.1016/0191-2615(82)90036-4

24. T. T. Shang, W. S. Jia, The GUS-property of linear complementarity problems over tensor spaces, *Optimization*, **75** (2026), 1831–1854. https://doi.org/10.1080/02331934.2025.2517324

25. N. Shimkin, A survey of uniqueness results for selfish routing, In: T. Chahed, B. Tuffin, *Network control and optimization*, Lecture Notes in Computer Science, Berlin, Heidelberg: Springer, 2007, 33–42. https://doi.org/10.1007/978-3-540-72709-5_4

26. J. Tidswell, A. Raith, Modelling traffic assignment objectives with emission cost functions, *Australasian Transport Research Forum (ATRF) 2017 Proceedings*, Auckland, New Zealand, 2017.

27. J. G. Wardrop, Some theoretical aspects of road traffic research, *Proceedings of the Institution of Civil Engineers, Part II*, **1** (1952), 325–362. https://doi.org/10.1680/ipeds.1952.11259

28. K. Wang, W. Jia, A new intelligent algorithm for solving generalized nash equilibrium problem, *Alex. Eng. J.*, **123** (2025), 17–28. https://doi.org/10.1016/j.aej.2025.03.044

AIMS Press